An optimal-fuzzy two-phase CLOS guidance law design using ant colony optimisation

H. Nobahari and S. H. Pourtakdoust
Department of Aerospace Engineering
Sharif University of Technology
Tehran, Iran

ABSTRACT

The well-known ant colony optimisation (ACO) meta-heuristic is applied to optimise the parameters of a new fuzzy command to line-of-sight (CLOS) guidance law. The new guidance scheme includes two phases, a midcourse and a terminal phase. In the first phase, a lead strategy is utilised which reduces the acceleration demands. A proportional derivative (PD) fuzzy sliding mode controller is used as the main tracking controller of the first phase. Moreover, a supervisory controller is coupled with the main tracking controller to guarantee the missile flight within the beam. In the terminal phase, a pure CLOS guidance law without lead angle is utilised. For this phase, a new hybrid fuzzy proportional-integral-derivative (PID) fuzzy sliding mode controller is proposed as a high precision tracking controller. The parameters of the proposed controllers for the first and the second phases are optimised using ACO. In this regard, the recently developed continuous ant colony system (CACS) algorithm is extended to multi-objective optimisation problems and utilised to optimise the parameters of the pre-constructed fuzzy controllers. The performance of the resulting guidance law is evaluated at different engagement scenarios and compared with the well-known feedback linearisation method. The comparison is also made in the presence of measurement noise.

NOMENCLATURE

A_1	the fuzzy set defined over time, corresponding to the first guidance phase
A_2	the fuzzy set defined over time, corresponding to the second guidance phase
$\bar{a}_c$	the average of control effort for given scenarios
$a_{c,max}$	maximum acceleration per channel
a_{mx}	axial acceleration of missile
a_{my}	yaw acceleration of missile
a_{mz}	pitch acceleration of missile
a_{ty}	yaw acceleration of target
a_{tz}	pitch acceleration of target
a_{yc}	yaw acceleration command
a_{zc}	pitch acceleration command
a_{yc_1}	the first phase yaw acceleration command
a_{yc_2}	the second phase yaw acceleration command
a_{zc_1}	the first phase pitch acceleration command
a_{zc_2}	the second phase pitch acceleration command
C_D	drag coefficient
C_{D_0}	zero lift drag coefficient
C_L	lift coefficient
Cθ	Cos(θ)
d_m	disturbance due to the difference between commanded and actual missile acceleration
d_t	disturbance due to real target manoeuvre
$d_{t'}$	disturbance due to virtual target manoeuvre
D	drag force
e_{max}	the centre of the fuzzy set positive (P) defined over the error signal
$\dot{e}_{max}$	the centre of the fuzzy set positive (P) defined over the error rate signal
f_c	guidance command frequency
g	gravity acceleration
I^*	the indicator function used to activate the supervisory controller
I	the indicator surface used to define I^*
k	number of ants
k	design vector used in the definition of the supervisory controller
K	the coefficient of induced drag term

Paper No. 3113. Manuscript received 6 June 2006, revised 9 January 2007, accepted 30 August 2007.

https://doi.org/10.1017/S0001924000004802 Published online by Cambridge University Press

K_d the derivative gain of the PID controller/surface
$K_{d,max}$ the centre of the fuzzy set big defined over K_d
K_i the integral gain of the PID controller/surface
$K_{i,max}$ the centre of the fuzzy set big defined over K_i
K_p the proportional gain of the PID controller/surface
$K_{p,max}$ the centre of the fuzzy set big defined over K_p
M missile mass
M mach number
NB the fuzzy set 'negative big'
NM the fuzzy set 'negative mid'
PB the fuzzy set 'positive big'
PM the fuzzy set 'positive mid'
ZO the fuzzy set 'zero'
$\bar{r}_n$ average of normalised tracking error for given scenarios
R_m tracker-to-missile range
R_t tracker-to-target range
s distance from the sliding surface
S fuzzy variable of the universe of discourse, s
$S_{1,\mathrm{NB}}$ centre of the fuzzy set *NB* defined over s corresponding to the first phase
$S_{1,\mathrm{PB}}$ centre of the fuzzy set *PB* defined over s corresponding to the first phase
$S_{1,\mathrm{PM}}$ centre of the fuzzy set *PM* defined over s corresponding to the first phase
$S_{2,\mathrm{PM}}$ centre of the fuzzy set *PM* defined over s corresponding to the second phase
Sθ Sin(θ)
S missile reference area
t_f total flight time
$t_{f,min}$ minimum flight time
t_{go} time-to-go
$t_{go,man}$ time-to-go at which target manoeuvres
$t_{go,min}$ minimum time-to-go
$t_{2,min}$ minimum time duration required for the second phase
t_S shaping phase time duration
T thrust force
u total control signal
u_M main control signal
u_S supervisory control signal
$U_{1,\mathrm{NB}}$ centre of the fuzzy set *NB* defined over u corresponding to the first phase
$U_{1,\mathrm{PB}}$ centre of the fuzzy set *PB* defined over u corresponding to the first phase
$U_{1,\mathrm{PM}}$ centre of the fuzzy set *PM* defined over u corresponding to the first phase
$U_{2,\mathrm{PM}}$ centre of the fuzzy set *PM* defined over u corresponding to the second phase
V Lyapunov function
v_m missile velocity
v_t target velocity
(x_m, y_m, z_m) missile position in inertial frame
(x_t, y_t, z_t) target position in inertial frame
(X_I, Y_I, Z_I) inertial frame
(X_L, Y_L, Z_L) line-of-sight (LOS) frame
(X_M, Y_M, Y_M) missile body frame
(X_T, Y_T, Z_T) target body frame
γ_m elevation angle of LOS to missile
γ_t elevation angle of LOS to target
δ beam half angle
ζ damping ratio of missile control system
η_1 scaling factor used to normalise s for the first phase
η_2 scaling factor used to normalise s for the second phase
θ_m pitch angle of missile
θ_t pitch angle of target
λ_M a positive constant used to define the sliding surface of the main controller
λ_S a positive constant used to define the indicator surface of the supervisory controller
μ membership function
ρ air density
σ_m azimuth angle of LOS to missile
σ_t azimuth angle of LOS to real target
$\sigma_{t'}$ azimuth angle of LOS to virtual target
σ_L azimuth lead angle
τ pheromone intensity
φ_a angle of target lateral manoeuvre measured from Y_T
φ_{mc} roll angle command
ψ_m yaw angle of missile
ψ_t yaw angle of target
ω_n natural frequency of missile control system

1.0 INTRODUCTION

The principle of command to line-of-sight (CLOS) guidance law is to force the missile to fly as nearly as possible along the instantaneous line joining the ground tracker and the target, called the line-of-sight (LOS)[1-21]. Theoretically, the missile-target dynamic equations are nonlinear and time-varying, partly because the equations of motion are described in an inertial frame, while aerodynamic forces and moments are prescribed in the missile and target body frames. Many different control techniques have been developed and applied to design CLOS guidance laws, examples of which are optimal control theory[6,10], feedback linearisation[7], polynomial method[8], variable structure control[9], supervisory control[11], fuzzy logic control[12-16] and so on.

The CLOS guidance is regarded as a simple and low-cost guidance concept primarily since it allows for the placement of avionics on the launch platform instead of the expendable vehicle[7]. The performance of CLOS guidance is known to be typically good for low speed targets[4]. But as the velocity of target increases, the LOS angular rate and acceleration increase as well. This means that in order for the missile to stay on the tracker beam, a CLOS missile must pull latax, leading to a curved trajectory. This demand for additional latax is sometimes supplied in the form of feed-forward signals. Moreover, as the range of target increases, it will be a challenge to compromise between miss distance and control effort. To reduce the acceleration demands for high speed targets, there is a well-known modification on CLOS guidance, called the lead angle method[4,5,19,20]. In this method, missile is guided toward a virtual target located with a lead angle with respect to the real target. However, this method needs a continuous and precise estimation of time-to-go. In this paper a combination of lead angle method and pure CLOS guidance is proposed to simultaneously receive the benefits of the two strategies. The proposed guidance scheme is composed of two sequential phases. In the first phase, namely the midcourse phase, the lead angle method is utilised to reduce the acceleration demands using approximate information on time-to-go. In the second phase, namely the terminal phase, a pure CLOS guidance, based on a precise tracking controller, is utilised to accurately intercept the target with no information requirement on time-to-go.

Noting to the recent advances in intelligent control systems and soft-computing technology, one can utilise fuzzy logic (FL) to design the first and the second phase controllers, as well as the shaping phase. The most attractive feature of fuzzy logic control (FLC) is that the expert knowledge can be easily incorporated into the design process. FLC can model the qualitative aspects of human knowledge and reasoning processes without employing precise quantitative analyses. It also possesses several advantages such as robustness, being model-free, universal approximation and a rule-based algorithm[14]. However, the stability analysis for general FLC systems is still lacking. To cope with this deficiency, a combination of FLC and the well-known sliding mode control (SMC) has been proposed in recent years, called fuzzy sliding mode control (FSMC)[23-25]. The stability of FSMC can be proved in the Lyapunov

https://doi.org/10.1017/S0001924000004802 Published online by Cambridge University Press

sense[25]. This technique has been widely used in many control applications, as well as the CLOS guidance problem[14]. The other advantage of FSMC is that it has fewer fuzzy rules than FLC. Moreover, by using SMC, the system possesses more robustness against parameter variations and external disturbances.

In this study PD-FSMC, known as a fast and coarse controller[26], is utilised for the midcourse phase. In addition a supervisory controller, as proposed in Ref. 11, is coupled with the main tracking controller to guarantee the missile flight within the beam. In the terminal phase a new hybrid fuzzy PID-FSMC is proposed, as a precise tracking controller. The proposed fuzzy PID-FSMC can be described as the fuzzy gain scheduling (FGS)[27] of a PID fuzzy sliding mode controller. A fuzzy shaping phase is also utilised to gradually switch from the first to the second guidance phase.

The designer should determine the parameters of the first and the second phase fuzzy controllers, as well as the shaping phase. In traditional FLC designs, the parameters were tuned by a trial and error procedure, based on certain physical sense or designer's experiences. However this tuning procedure is faced with two important problems; the knowledge does not always completely exist and the manual tuning of all the base parameters takes time. To cope with these problems, the learning methods were introduced. The first attempt was made by Procyk and Mamdani in 1979, with a self tuning controller[28]. The gradient descent method was used by Takagi and Sugeno in 1985 as a learning tool for fuzzy modeling and identification[29]. It was used by Nomura, *et al* in 1991 as a self tuning method for fuzzy control[30].

The gradient descent method is appropriate for simple problems and real time learning, since it is fast. But it may be trapped into local minima. Also the calculation of the gradients depends on the shape of membership functions employed, the operators used for fuzzy inferences, as well as the selected cost function. In 1998, Siarry and Guely applied the well-known genetic algorithm to the problem of tuning the parameters of a Takagi-Sugeno fuzzy rule base[31]. The same problem was solved in Ref. 32, using continuous ant colony system (CACS)[33], which is a variant of the well-known ant colony optimisation (ACO) meta-heuristic[34,35] for continuous optimization problems. CACS is known as a fast global optimisation method, as compared to some other meta-heuristics such as genetic algorithms (GA)[32,33].

In a previous work[16], the authors have successfully applied CACS to design a PD-FSMC CLOS guidance law. In this study, CACS is utilised to design the proposed two-phase CLOS guidance scheme. The design parameters include the parameters of the first and the second phase fuzzy controllers, as well as the shaping phase. The optimisation problem is to find the optimum value of the design parameters that simultaneously minimise the control effort of the total flight, as well as the average tracking error of the terminal phase. This is a multi-objective optimisation problem. So CACS is modified and extended from single to multi-objective optimisation problems. The cost functions are evaluated over ten randomly generated engagement scenarios. In the simulation of these scenarios, a step target manoeuvre[3] with random direction and random initiation time is used. The performance of the optimal two-phase CLOS guidance strategy, designed in this way, is then evaluated at some other engagement scenarios and compared with that of a model-based feedback linearisation method, proposed in Ref. 7. The simulation results show good performances both in terms of control effort and tracking behaviour, as well as the final miss distance.

2.0 PROBLEM DEFINITION

In this section the three-dimensional CLOS guidance is formulated as a nonlinear time varying tracking problem. In modeling the pursuit dynamics of missile and target, the following assumptions are made:

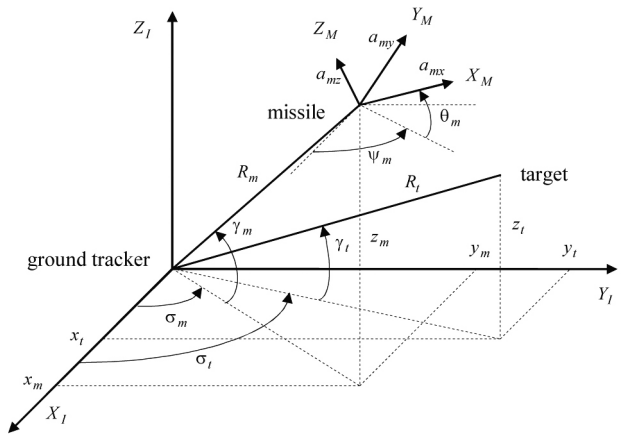

Figure 1. Three-dimensional pursuit situation.

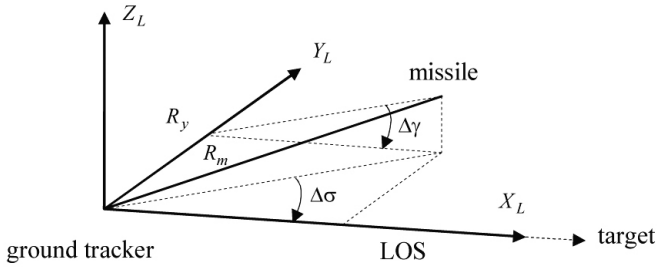

Figure 2. Definition of the tracking error.

A1: Compared with the overall guidance loop, the autopilot dynamics is fast enough to be neglected.
A2: The total angle-of-attack is small enough to be neglected.
A3: The body-beam angle is small enough to be neglected.

These assumptions are generally accepted in the design and analysis of missile guidance laws. However, the effect of autopilot dynamics and body-beam angle on guidance performance and the effect of angle-of-attack on induced drag are considered in the simulations.

The three-dimensional pursuit situation is depicted in Fig. 1, where the origin of the inertial frame is located at the ground tracker. The z_I axis is vertical upward and the X_1–Y_1 plane is tangent to the Earth surface. The origin of the missile body frame is fixed at the missile centre of mass with the X_M axis forward along the missile centreline.

By defining the LOS frame as depicted in Fig. 2, the three-dimensional guidance problem can be converted to a tracking problem. As mentioned in section 1, the concept of CLOS guidance law is to guide the missile onto the LOS to target. Therefore a reasonable choice of the tracking error can be considered as follows

$$\begin{bmatrix} \Delta\sigma \\ \Delta\gamma \end{bmatrix} = \begin{bmatrix} \sigma_m - \sigma_t \\ \gamma_m - \gamma_t \end{bmatrix} \quad \ldots (1)$$

The problem involves designing a controller to drive $[\Delta\sigma, \Delta\gamma]^\tau$ to zero. The same design algorithm will be applied for both azimuth and elevation angle control. In the following, the azimuth angle control is chosen as an example.

Assume that $e(t) = \Delta\sigma$ represents the azimuth loop tracking error. By considering a_m and a_t as the missile's and the target's acceleration along the axis Y_L, it can easily be shown that

$$\begin{aligned} \ddot{\sigma}_t &= -2(\dot{R}_t / R_t)\dot{\sigma}_t + a_t / R_t \\ \ddot{\sigma}_m &= -2(\dot{R}_m / R_m)\dot{\sigma}_m + a_m / R_m \end{aligned} \quad \ldots (2)$$

https://doi.org/10.1017/S0001924000004802 Published online by Cambridge University Press

Therefore, the differential equation of the error signal can be written as

$$\ddot{e}(t) = -2(\dot{R}_m / R_m)\dot{e}(t) - 2(\dot{R}_m / R_m)\dot{\sigma}_t(t) - \ddot{\sigma}_t + (1/R_m)\,q_m \quad \ldots (3)$$

By defining $f(\mathbf{e},t) = -2(\dot{R}_m/R_m)\dot{e}(t)$ and $g(t) = 1/R_m(t)$, Equation (3) can be rewritten as

$$\begin{aligned}\ddot{e}(t) &= f(\mathbf{e},t) + g(t)[a_m(t) - a_{yc}(t) + a_{yc}(t) - R_m\ddot{\sigma}_t - 2\dot{R}_m\dot{\sigma}_t] \\ &= f(\mathbf{e},t) + g(t)[u(t) + d_m(t)]\end{aligned} \quad \ldots (4)$$

where $\mathbf{e} = [e(t), \dot{e}(t)]^T$ is the state vector of the error signal, $u(t) = a_{yc}(t) - R_m\ddot{\sigma}_t - 2\dot{R}_m\dot{\sigma}_t$ is the control signal and $d_m(t) = a_m - a_{yc}(t)$ the disturbance due to the difference between the commanded acceleration and the actual acceleration, respectively. The equation $a_{yc}(t) = u(t) + R_m\ddot{\sigma}_t + 2\dot{R}_m\dot{\sigma}_t$ shows that the feed-forward term $R_m\ddot{\sigma}_t + 2\dot{R}_m\dot{\sigma}_t$ can be added to the control signal $u(t)$, obtained from the guidance loop, to make the acceleration command $a_{yc}(t)$. The use of this feed-forward term usually entails additional measurements and/or differentiations.

3.0 TWO-PHASE CLOS GUIDANCE

The performance of CLOS guidance is known to be typically good for low speed targets. But as the velocity of target increases, the LOS angular rate and acceleration increase as well. This means that in order for the missile to stay on the tracker beam, a CLOS missile must pull latax, leading to a curved trajectory. In the case of high crossing rate targets, the CLOS guidance law with lead angle can be utilised. In this strategy, missile is guided toward a virtual target located with a lead angle with respect to the real target. The lead angle decreases with time and becomes zero at the interception point. This strategy decreases the curvature of missile trajectory as well as the demanded acceleration commands. However, to calculate the lead angle it is necessary to continuously estimate time-to-go (t_{go}) with an acceptable accuracy. But in the condition of prevailing electronic counter measures (ECM) it is not possible to measure the range of target and estimate t_{go}. As a result the lead strategy can not be used in such a condition.

Although the exact value of t_{go} is not always known, a lower bound, called the minimum time-to-go ($t_{go,min}$), can easily be estimated using any information on the initial range and velocity of target. To calculate $t_{go,min}$, the minimum interception time is used instead of the exact value of this parameter ($t_{go,min} = t_{f,min} - t$). Therefore no additional measurement is needed. Then, the guidance problem can be divided into two separate phases. In the first phase, namely the midcourse phase, the CLOS guidance law with lead angle can be applied based on the initially estimated $t_{f,min}$ instead of the instantaneous t_f. In the second phase, namely the terminal phase, the ordinary CLOS guidance law is applied with no information requirement on the time-to-go. The start time of the terminal phase must be sufficiently less than $t_{f,min}$ to provide the minimum time required for this phase to become effective ($t_{2,min}$). This parameter is determined by the optimisation algorithm such that in the worst condition which the interception time equals to the initially estimated $t_{f,min}$, the missile can successfully intercept the target.

Since the proposed guidance law has two phases, a shaping phase is also necessary to gradually change the guidance strategy. In this paper a single input single output TSK fuzzy system is proposed for the shaping phase. The input and output of this fuzzy system are time and acceleration command, respectively. Two fuzzy sets A_1 and A_2 are defined over the input variable, corresponding to the first and the second guidance laws. These sets are shown in Fig. 3.

The shaping phase duration, t_S, can also be determined by the optimisation algorithm. To continuously switch from the first to the second phase, it is recommended to use Z and S membership functions instead of the common trapezoidal ones. The membership

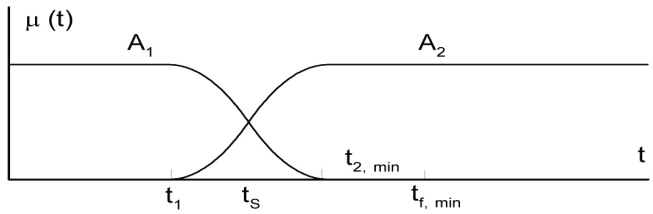

Figure 3. Definition of the fuzzy sets for the shaping phase fuzzy system.

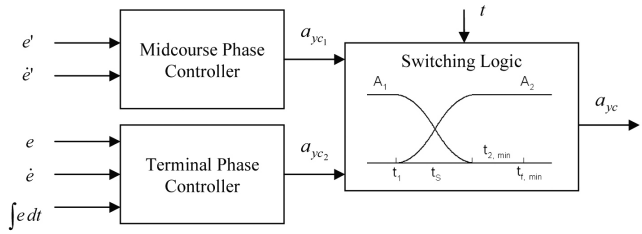

Figure 4. The implementation model of two-phase CLOS guidance for azimuth channel.

functions of the corresponding fuzzy sets A_1 and A_2 are defined as follows

$$\mu_{A_1}(t) = \begin{cases} 1 & t < t_1 \\ 0.5 + 0.5\,\mathrm{Cos}\left(\dfrac{t - t_1}{t_S}\pi\right) & t_1 < t < t_{f,min} - t_{2,min} \\ 0 & t > t_{f,min} - t_{2,min} \end{cases} \quad \ldots (5)$$

$$\mu_{A_2}(t) = \begin{cases} 0 & t < t_1 \\ 0.5 - 0.5\,\mathrm{Cos}\left(\dfrac{t - t_1}{t_S}\pi\right) & t_1 < t < t_{f,min} - t_{2,min} \\ 1 & t > t_{f,min} - t_{2,min} \end{cases} \quad \ldots (6)$$

where t_S, called the shaping phase duration, is also determined by the optimisation algorithm. It can be easily shown that $\mu_{A_1}(t) + \mu_{A_2}(t) = 1$, for all $t \geq 0$. The fuzzy control rules of the shaping phase are written as follows:

Rule 1: if t is A_1, then $a_{yc} = a_{yc_1}$, $a_{zc} = a_{zc_1}$
Rule 2: if t is A_2, then $a_{yc} = a_{yc_2}$, $a_{zc} = a_{zc_2}$

Defuzzification of the system output is accomplished by the method of centre-of-gravity. In this way, the instantaneous acceleration command can be written as follows:

$$\begin{aligned} a_{yc} &= \mu_{A_1}(t)\,a_{yc_1} + \mu_{A_2}(t)\,a_{yc_2} \\ a_{zc} &= \mu_{A_1}(t)\,a_{zc_1} + \mu_{A_2}(t)\,a_{zc_2} \end{aligned} \quad \ldots (7)$$

The implementation model of the two-phase CLOS guidance for a sample channel is shown in Fig. 4. In the next two sections the proposed controllers for the midcourse and the terminal phases are described.

4.0 MIDCOURSE GUIDANCE LAW DESIGN

The main objective of the first guidance phase is to guide the missile along an optimally generated trajectory toward the target. In this regard, the CLOS guidance with lead angle is utilised as an alter-

https://doi.org/10.1017/S0001924000004802 Published online by Cambridge University Press

native. This strategy decreases the curvature of missile trajectory with respect to the pure CLOS guidance. It also decreases the total acceleration requirement as well as the total time of flight. A fuzzy sliding mode controller is constructed, as the main tracking controller of this phase, to guide the missile along the desired LOS. Moreover the proposed supervisory controller in Ref. 11 is used to guarantee the missile flight within the beam. This supervisory controller is applied in the form of an additional control signal that is activated when the beam angle constraint goes to be violated. In the next subsections, the proposed main and supervisory controllers are described.

4.1 Design of the main tracking controller

The main tracking controller of the first guidance phase is designed to approximately guide the missile on the virtual LOS. Here, the error signal is defined as $e'(t) = \sigma_t' - \sigma_m$. In this phase, it is not important to have a precise and fast tracking controller since the interception is not supposed to occur. However it is important to have no overshoot or only a small overshoot because missile may be occasionally guided near the beam boundaries. Therefore, in this paper a proportional derivative (PD) fuzzy sliding mode controller (FSMC) is proposed as the main tracking controller of the first phase. This controller is described in the next subsections.

4.1.1 Sliding mode control

Let $s(\mathbf{e}')$ = 0 denote a hyper-surface in the space of the error state, called the sliding surface. The purpose of sliding mode control is to force the error vector $\mathbf{e}'$ to approach the sliding surface and then move along it to the origin. If A PD sliding surface s is defined as

$$s(e',\dot{e}') = \left(\frac{\mathrm{d}}{\mathrm{d}t} + \lambda_M\right)\mathbf{e}' = \dot{\mathbf{e}}' + \lambda_M\,\mathbf{e}' \qquad \ldots (8)$$

where λ_M is a positive constant that is determined by the optimisation algorithm. It is obvious from Equation (8) that keeping the states of system on the sliding surface will guarantee the tracking error vector asymptotically approach to zero. The corresponding sliding condition[36] is

$$\frac{1}{2}\frac{\mathrm{d}}{\mathrm{d}t}s^2 = s\dot{s} \le 0 \qquad \ldots (9)$$

The general control structure that satisfies the stability of the sliding motion, can be written as[36]

$$u_M = \hat{u}_M - \mathrm{K}\,\mathrm{sgn}(s) \qquad \ldots (10)$$

where $\hat{u}_M$ is called the equivalent control law that is derived by setting $s = \dot{s} = 0$, and K is a positive constant. The sliding condition can be satisfied as long as each K is chosen large enough[36].

4.1.2 Fuzzy sliding mode control

FSMC can be regarded as a fuzzy regulator that controls the state of system to approach to the sliding surface. Let S denote the fuzzy variable of the universe of discourse, s. Then some linguistic terms can be defined to describe the fuzzy variable S, such as zero (ZO), positive big (PB), negative mid (NM), etc. Such linguistic expressions can be used to form fuzzy control rules as follows

Rule 1: If S is NB, then U_M is PB
Rule 2: If S is NM, then U_M is PM
Rule 3: If S is ZO, then U_M is ZO
Rule 4: If S is PM, then U_M is NM
Rule 5: If S is PB, then U_M is NB
. . . (11)

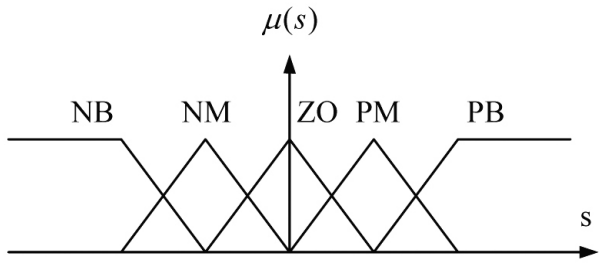

Figure 5. Definition of fuzzy membership functions for the main controller of the first phase.

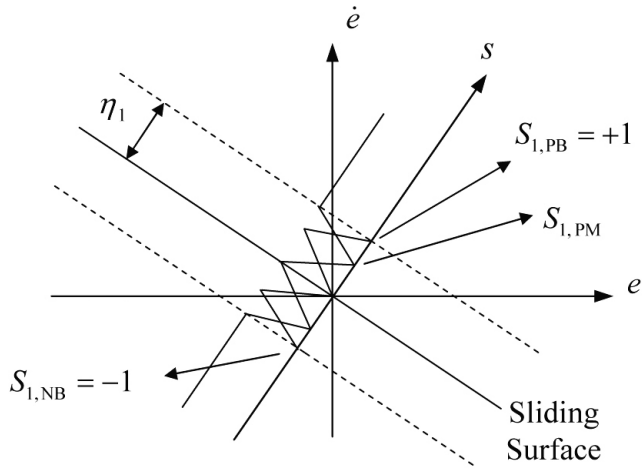

Figure 6. Fuzzy sliding surface of a second order system.

where U_M denotes the fuzzy variable of the control signal u. Each linguistic term is associated with a fuzzy set as shown in Fig. 5. The parameters of these sets are determined by the optimisation algorithm. A scaling factor is also used to normalise the fuzzy sets.

The fuzzy sliding surface of a second-order system is shown in Fig. 6, where η_1 represents the scaling factor. For normalised fuzzy sets, $S_{1,\mathrm{NB}} = -1$ and $S_{1,\mathrm{PB}} = 1$. The maximum control energy u_{max} is also bounded by physical limitations, that is $U_{1,\mathrm{NB}} = -1$ and $U_{1,\mathrm{PB}} = 1$. If the symmetry of fuzzy terms corresponding to s and U_M is assumed, the remaining design factors are $S_{1,\mathrm{PM}}$, $U_{1,\mathrm{PM}}$, and the scaling factor η_1. Therefore, the optimisation parameters corresponding to the main controller of the first phase include $S_{1,\mathrm{PM}}$, $U_{1,\mathrm{PM}}$, η_1, and the positive constant λ_M.

4.2 Design of the supervisory controller

The lead angle method, used in the midcourse phase, may occasionally guide the missile near the boundaries of the tracking beam. The purpose of the supervisory controller is to guarantee the missile to fly within the beam. Here, the guidance problem involves designing a controller that controls the signal $u(t)$ to drive $e(t)$ to its desired value, subjected to the following constraints

$$\begin{cases} \ddot{e} = f(\mathbf{e},t) + g(t)[u(t) + d_m(t)] \\ |e(t)| < \delta \quad \text{for all} \quad t \ge 0 \end{cases} \qquad \ldots (12)$$

where δ is the beam half angle. The first constraint is the dynamic equation of system and the second one is the beam angle constraint. The control signal $u(t)$ is proposed as a combination of the main and the supervisory controller. It can be written as follows

$$u(t) = u_M + \Gamma^* u_S \qquad \ldots (13)$$

https://doi.org/10.1017/S0001924000004802 Published online by Cambridge University Press

The main controller, u_M, tracks the desired value, $e_d(t)$, while the supervisory controller, u_S, acts to satisfy the beam constraint. The supervisory controller is activated only when the controlled signal $e(t)$ goes to hit the boundary of the constraint set $\{e: |e| < \delta\}$. The indicator function I^* is defined as follows

$$I^* = \begin{cases} 0 & |e| < \delta \\ 1 & |\varepsilon| \geq \delta \end{cases} \quad \ldots (14)$$

Therefore u_M is still the main control action. The problem now is to design the control signal u_S such that $|e(t)| < \delta$ for all $t > 0$. Let's define $u^*(t)$ as follows:

$$u^*(t) = \frac{1}{g(t)}\left[-f(\mathbf{e},t) - \mathbf{k}^{\mathrm{T}}\mathbf{e}\right] \quad \ldots (15)$$

where $\mathbf{k} = [k_1\ k_2]^{\mathrm{T}} \in \Re^2$ is such that all roots of the equation $S^2 + k_2 S + k_1 = 0$ are in the left half of the complex plane. Using Equations (13) and (15), one can rewrite the Equation (4) as follows:

$$\ddot{e}(t) = -\mathbf{k}^{\mathrm{T}}\mathbf{e} + g(t)[u_M - u^* + I^* u_S + d_m(t)] \quad \ldots (16)$$

Defining

$$\mathbf{\Lambda} = \begin{bmatrix} 0 & 1 \\ -k_1 & -k_2 \end{bmatrix} \quad , \quad \mathbf{b} = \begin{bmatrix} 0 \\ g(t) \end{bmatrix}$$

allows the Equation (16) to be written as:

$$\dot{\mathbf{e}} = \mathbf{\Lambda}\mathbf{e} + \mathbf{b}[u_M - u^* + I^* u_S + d_m(t)] \quad \ldots (17)$$

Now the supervisory controller u_S is designed to guarantee the situation $|e(t)| < \delta$. A candidate Lyapunov function can be defined as:

$$V = \frac{1}{2}\mathbf{e}^{\mathrm{T}}\mathbf{P}\mathbf{e} \quad \ldots (18)$$

where $\mathbf{P}$ is a symmetric positive definite matrix satisfying the Lyapunov equation

$$\mathbf{\Lambda}^{\mathrm{T}}\mathbf{P} + \mathbf{P}\ddot{\mathbf{E}} = -\mathbf{Q} \quad \ldots (19)$$

and the positive definite matrix $\mathbf{Q} > 0$ is specified by the designer. Since $\mathbf{\Lambda}$ is stable, such $\mathbf{P}$ always exists. Using Equations (17) and (19) and considering $|e| \geq \delta$, we will have:

$$\begin{aligned} \dot{V} &= \frac{1}{2}\mathbf{e}^{\mathrm{T}}\mathbf{P}\mathbf{\Lambda}\mathbf{e} + \frac{1}{2}\mathbf{e}^{\mathrm{T}}\mathbf{P}\mathbf{b}[u_M - u^* + u_S + d_m(t)] \\ &\quad + \frac{1}{2}\mathbf{e}^{\mathrm{T}}\mathbf{\Lambda}^{\mathrm{T}}\mathbf{P}\mathbf{e} + \frac{1}{2}[u_M - u^* + u_S + d_m(t)]\mathbf{b}^{\mathrm{T}}\mathbf{P}\mathbf{e} \\ &= -\frac{1}{2}\mathbf{e}^{\mathrm{T}}\mathbf{Q}\mathbf{e} + W \end{aligned} \quad \ldots (20)$$

where the first term is always negative and

$$W = \mathbf{e}^{\mathrm{T}}\mathbf{P}\mathbf{b}\,[u_M - u^* + u_S + d_m(t)] \quad \ldots (21)$$

Considering d_m^u as the upper limit of d_m

$$W \leq \left|\mathbf{e}^{\mathrm{T}}\mathbf{P}\mathbf{b}\right| \cdot \left(|u_M| + |u^*| + d_m^u\right) + \mathbf{e}^{\mathrm{T}}\mathbf{P}\mathbf{b}\,u_S \quad \ldots (22)$$

We also need some additional information about $f(\mathbf{e},t)$ and $g(t)$. One can determine $f^u(\mathbf{e},t)$ and $g_L(t)$ such that $|f(\mathbf{e},t)| \leq f^u(\mathbf{e},t)$ and $0 < g_L(t) < g(t)$. That is, we assume that we know the upper bound of $f(\mathbf{e},t)$ and the lower bound of $g(t)$. Now u_s is proposed as follows:

$$u_S = -\operatorname{sgn}(\mathbf{e}^{\mathrm{T}}\mathbf{P}\mathbf{b}) \cdot \left[\frac{1}{g_L(t)}\left(f^u(\mathbf{e},t) + \left|\mathbf{k}^{\mathrm{T}}\mathbf{e}\right|\right) + |u_M| + d_m^u\right] \quad \ldots (23)$$

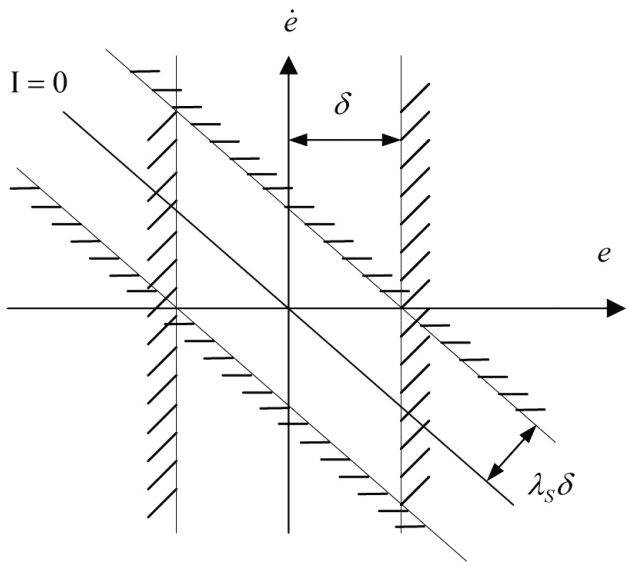

Figure 7. Definition of indicator surface in phase plane.

Therefore

$$W \leq \left|\mathbf{e}^{\mathrm{T}}\mathbf{P}\mathbf{b}\right| \cdot \left(|u_M| + \frac{|f(\mathbf{e},t)| + \left|\mathbf{k}^{\mathrm{T}}\mathbf{e}\right|}{g(t)} + d_m^u - \frac{f^u(\mathbf{e},t)}{g_L(t)} - \frac{\left|\mathbf{k}^{\mathrm{T}}\mathbf{e}\right|}{g_L(t)} - |u_M| - d_m^u \right)$$

$$W \leq \left|\mathbf{e}^{\mathrm{T}}\mathbf{P}\mathbf{b}\right| \cdot \left(\frac{|f(\mathbf{e},t)|}{g(t)} - \frac{f^u(\mathbf{e},t)}{g_L(t)} + \frac{\left|\mathbf{k}^{\mathrm{T}}\mathbf{e}\right|}{g(t)} - \frac{\left|\mathbf{k}^{\mathrm{T}}\mathbf{e}\right|}{g_L(t)} \right) \leq 0$$

According to Equation (20), the last inequality implies $\dot{V} < 0$. Therefore the supervisory controller[23] stabilises the system in the sense of Lyapunov and guarantees that $|e|$ will decrease if $|e| \geq \delta$. Since it is required to absolutely prevent the situation that $|e| \geq \delta$, in the next step we define an indicator surface, I;

$$I = \dot{e} + \lambda_S e \quad \ldots (24)$$

where λ_S is specified by the designer. The so defined indicator surface has been shown in Fig. 7. It can easily be observed that to satisfy the condition $|e| < \delta$, it is also necessary to control I such that

$$|I| < \lambda_S \delta \quad \ldots (25)$$

Therefore the definition of indicator function can be modified as follows:

$$I^* = \begin{cases} 0 & |e| < \delta \ \textit{and}\ |I| < \lambda_S\delta \\ 1 & |e| \geq \delta \ \textit{or}\ |I| \geq \lambda_S\delta \end{cases} \quad \ldots (26)$$

Since I^* in Equation (26) is a step function, the supervisory controller begins operation as soon as e hits the boundary $|e| = \delta$ or I hits the boundary $|I| = \lambda_S\delta$, and is idle while e and I satisfy the constraint sets $|e| < \delta$ and $|I| < \lambda_S\delta$, hence the system may oscillate across the boundary $|I| = \lambda_S\delta$. One way to overcome this chattering problem is to allow I^* to continuously changing from 0 to 1. So a modification to I^* is proposed as follows:

$$I^* = \begin{cases} 0 & |e| < a\delta \ \text{ and } \ |I| < a\lambda_S\delta \\ \dfrac{\max\left(|e|/\delta, |I|/\lambda_S\delta\right) - a}{1-a} & a\delta \leq |e| < \delta \ \text{ or } \ a\lambda_S\delta \leq |I| < \lambda_S\delta \\ 1 & |e| \geq \delta \ \text{ or } \ |I| \geq \lambda_S\delta \end{cases} \quad \ldots (27)$$

where $a \in (0,1)$ is a parameter specified by designer. With this

https://doi.org/10.1017/S0001924000004802 Published online by Cambridge University Press

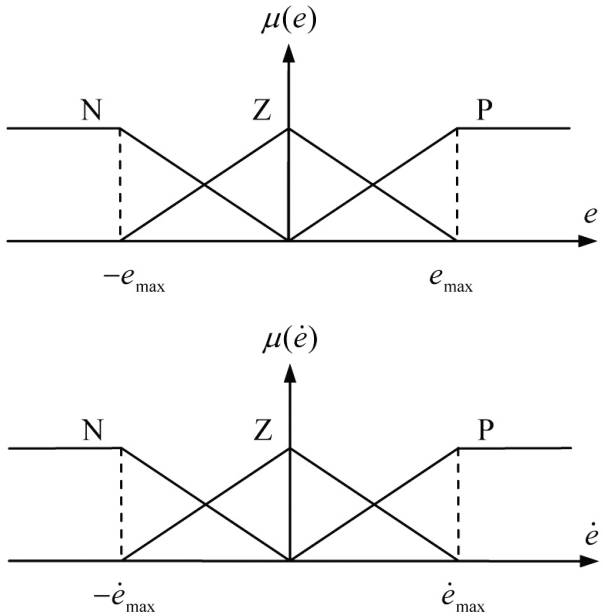

Figure 8. Definition of membership functions for the inputs of the fuzzy gain scheduler.

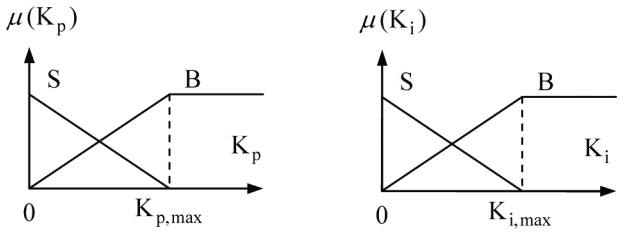

Figure 9. Definition of membership functions for the outputs of the fuzzy gain scheduler.

modified I^* in Equation (27), the supervisory controller u_S operates continuously from zero to full strength as $|e|/\delta$ or $|I|/\lambda_s\delta$ changes from a to 1.

5.0 TERMINAL GUIDANCE LAW DESIGN

In the terminal phase, the pure CLOS guidance law without lead angle is utilised. The guidance problem involves designing a controller to drive $[\Delta\sigma, \Delta\gamma]^T$ to zero. The main objective of the terminal phase is to intercept the target with a low miss distance. Therefore, a fast and fine tracking controller should be designed. For this purpose, a new hybrid fuzzy PID-FSMC is proposed. The proposed scheme can be described as the fuzzy gain scheduling[27] of a PID fuzzy sliding mode controller. In the next two subsections, the concept of fuzzy PID-FSMC is described.

5.1 Fuzzy gain scheduling of PID controllers

Proportional integral derivative (PID) controllers are widely used in industrial control systems because of their simple structure and robust performance. The transfer function of a PID controller has the following form:

$$G(S) = K_p + K_i / S + K_d S \quad \ldots (28)$$

where K_p, K_i, and K_d are the proportional, integral and derivative gains, respectively. It is assumed that these parameters are in prescribed ranges [0, $K_{p,max}$], [0, $K_{i,max}$], and [0, $K_{d,max}$], respectively. Great efforts have been devoted to develop methods to determine optimal values of proportional, integral and derivative gains. Fuzzy gain scheduling of PID controllers was proposed by Zhao *et al*[27] in 1993. This method utilises a supervisory fuzzy system to determine the PID controller gains and it is the PID controller that generates the main control signal.

Human expertise on PID gain scheduling is used to exploit fuzzy rules. For example when there is a big error, a big control signal is required to achieve a fast rise time. To produce a big control signal, the PID controller should have a large proportional gain, a large integral gain, and a small derivative gain. Thus the proportional and integral gains (K_p, K_i) can be represented by the fuzzy set big (B), and the derivative gain by a fuzzy set small (S). The other situations are also investigated in the same manner and a thus complete rule base is developed corresponding to each output of the fuzzy system.

Table 1
Fuzzy gain scheduler rule base corresponding to K_p

$e/\dot{e}$	N	Z	P
N	B	B	B
Z	S	B	S
P	B	B	B

Table 2
Fuzzy gain scheduler rule base corresponding to K_i

$e/\dot{e}$	N	Z	P
N	S	S	S
Z	B	B	B
P	S	S	S

Table 3
Fuzzy gain scheduler rule base corresponding to K_d

$e/\dot{e}$	N	Z	P
N	B	B	B
Z	S	B	S
P	B	B	B

5.2 Fuzzy PID-FSMC

A general PID sliding surface can be defined as follows[14]

$$s = K_p\, e + K_i \int_{t_0}^{t} e\, dt + K_d\, \dot{e} \quad \ldots (29)$$

where $t_0 = t_{f,min} - t_{2,min}$ is the start time of the terminal phase. The PID-FSMC is regarded as a fuzzy regulator that controls the variable s approach to zero. The same membership functions as in Fig. 5 and the same fuzzy rules as proposed in Equation (11), are also adopted here.

In fuzzy PID-FSMC, the proportional, integral and derivative gains of the PID sliding surface are adapted on-line using a fuzzy gain scheduler as described in the previous subsection. The corresponding input and output membership functions are shown in Figs 8 and 9, respectively. The rule bases are provided in Tables 1, 2, and 3, corresponding to the outputs K_p, K_i, and K_d, respectively. Here, the product operator is chosen as t-norm, and the defuzzification is done using the method of centre of gravity.

The parameters of fuzzy PID-FSMC are determined through the optimisation process. Assuming $K_{d,max} = 1$, the remaining parameters include $S_{2,PM}$, $U_{2,PM}$, η_2, $K_{p,max}$, $K_{i,max}$, e_{max} and $\dot{e}_{max}$. The definitions of the first three parameters are similar to those of the main PD-FSMC tracking controller of the first phase.

https://doi.org/10.1017/S0001924000004802 Published online by Cambridge University Press

6.0 ANT COLONY OPTIMISATION META-HEURISTIC

Ant algorithms were inspired by the observation of the real ant colonies. An important and interesting behaviour of ant colonies is their foraging behaviour, and in particular, how ants can find the shortest path without using visual cues. While walking from the food sources to the nest and *vice versa*, ants deposit on the ground a chemical substance called pheromone which makes a pheromone trail. Ants use pheromone trails as a medium to communicate with each other. They can smell pheromone and when they choose their way, they tend to choose paths with more pheromone. The pheromone trail allows the ants to find their way back to the food source or to the nest. Also, the other ants can use it to find the location of the food sources, which are previously found by their nest mates.

6.1 Ant colony system

Ant colony system (ACS) is one of the first discrete algorithms, proposed based on ACO. At first it was applied to the well-known traveling salesman problem (TSP), which is a discrete optimisation problem. This algorithm uses a graph representation, like as the cities and the connections between them in the TSP. But, in addition to the cost measure, each edge has also a desirability measure, called pheromone intensity. To solve the problem, each ant generates a complete tour by choosing the nodes according to a so called pseudo-random-proportional state transition rule, which has two major features. Ants prefer to move to the nodes, which are connected by the edges with a high amount of pheromone, while in some instances, their selection may be completely random. The first feature is called exploitation and the second is a kind of exploration. While constructing a tour, ants also modify the amount of pheromone on the visited edges by applying a local updating rule. It concurrently simulates the evaporation of the previous pheromone and the accumulation of the new pheromone deposited by the ants while they are building their solutions. Once all the ants have completed their tours, the amount of pheromone is modified again, by applying a global updating rule. Again a part of pheromone evaporates and all edges that belong to the global best tour, receive additional pheromone conversely proportional to their length.

6.2 Continuous ant colony system

In this part, continuous ant colony system (CACS) is shortly introduced. The interested readers can refer to Ref. 32 and Ref. 33, to find more details.

A continuous optimisation problem is defined as finding the absolute minimum of a positive non-zero continuous cost function $f(x)$, within a given interval $[a,b]$, which the minimum occurs at a point x. In general f can be a multi-variable function, defined on a subset of $\Re^n$ delimited by n intervals $\{[a_i, b_i], i = 1, \ldots n\}$.

Continuous ant colony system (CACS) has all the major characteristics of ACS, but certainly in a continuous frame. These are a pheromone distribution model, a state transition rule, and a pheromone updating rule.

6.2.1 Continuous pheromone model

Although pheromone distribution has been first modeled over discrete sets, like the edges of TSP, in the case of real ants, pheromone deposition occurs over a continuous space. The pheromone intensity of CACS is modeled in the form of a normal probability distribution function (PDF):

$$\tau(x) = \frac{1}{\sqrt{2\pi}\sigma} e^{-\frac{(x-x_{\min})^2}{2\sigma^2}} \qquad \ldots (30)$$

where x_{min} is the best point in the interval $[a, b]$ which has been found from the beginning of the trial and σ is an index of the ants aggregation around x_{min}.

6.2.2 State transition rule

The pheromone intensity of CACS is modeled in the form of a normal PDF. Therefore a random generator with a normal PDF is used as the state transition rule to choose the next point to move to.

6.2.3 Pheromone update

Ants choose their way through the probabilistic strategy of Equation (30). At the first iteration, there isn't any knowledge about the minimum point and the ants choose their destinations only by exploration. It means that they must use a high value of σ, associated with an arbitrary x_{min}, to approximately model a uniform distribution function. During any iteration, pheromone distribution over the search space will be updated using the acquired knowledge of the evaluated points by the ants. This process gradually increases the exploitation behaviour of the algorithm, while its exploration behaviour will decrease. Pheromone updating can be stated as follows: The value of objective function is evaluated for the new selected points by the ants. Then, the best point found from the beginning of the trial is assigned to x_{min}. This is called global minimum update. Also the value of σ is updated based on the evaluated points during the last iteration and the aggregation of those points around x_{min}. To satisfy simultaneously the fitness and aggregation criteria, a concept of weighted variance is utilised as follows:

$$\sigma^2 = \frac{\sum_{j=1}^{k} \frac{1}{f_j - f_{min}} (x_j - x_{min})^2}{\sum_{j=1}^{k} \frac{1}{f_j - f_{min}}}, \text{ for all } j \text{ in which } f_j \neq f_{min} \qquad \ldots (31)$$

Here k is the number of ants. It means that the centre of region discovered during the subsequent iteration is the last best point and the narrowness of its width is dependent on the aggregation of the other competitors around the best one. The closer the better solutions get (during the last iteration) to the best one, the smaller is assigned to the next iteration.

6.3 Pareto continuous ant colony system

The original CACS, proposed in Ref. 32 has been developed for single objective optimisation problems. In this paper, the Pareto optimality condition (POC) is used to extend CACS to multi-objective optimisation problems. The proposed scheme is called Pareto CACS (PCACS).

POC is defined as follows[37]: Consider a problem with m different objective functions $f_1(\mathbf{x})$, ..., $f_m(\mathbf{x})$ and consider two different objective sets $\mathbf{f}^1$ and $\mathbf{f}^2$, corresponding to two feasible solutions $\mathbf{x}^1$ and $\mathbf{x}^2$. The objective set $\mathbf{f}^1$ is called Pareto optimal with respect to $\mathbf{f}^2$, if $f_j^1 \leq f_j^2$ for and $j = 1, \ldots, m$ for at least one j.

PCACS differs from the original CACS in the way pheromone distributions are updated. This method utilises two different Global minimum update (GMU) strategies, a Pareto GMU and a single objective GMU. Consequently, there are two current solutions corresponding to any iteration, a Pareto optimal solution ($\mathbf{x}_{min,p}$, $\mathbf{f}_{min,p}$), and a single objective optimal solution ($\mathbf{x}_{min,so}$, $\mathbf{f}_{min,so}$). At the beginning, these two solutions are the same. During iterations, the Pareto solution is replaced with a newly found solution, if POC is satisfied for the new solution. This is called Pareto GMU. The Pareto solution found after the final iteration is passed as the final solution of the multi-objective optimisation problem.

The single objective GMU is applied to each objective function independently from the others. This process can be stated as follows:

https://doi.org/10.1017/S0001924000004802 Published online by Cambridge University Press

At first the search space should be divided into m different subspaces E_1, ..., E_m, corresponding to the objective functions f_1, ..., f_m, respectively. The one-dimensional subspace $x_1(i = 1, \ldots n)$ is grouped in subspace $E_j(j = 1, \ldots m)$ if any change in x_1 has the most effect on the objective function f_j rather than the others. This grouping procedure is a part of problem definition and should be done before the optimisation process. During iterations, the current single-objective optimal solution ($\mathbf{x}_{min,so}$, $\mathbf{f}_{min,so}$) is replaced with a new found solution (x_j, f_j) if $f_j < f_{j,min,so}$. This criterion is checked for all objective functions. This is called single objective GMU.

At the end of any iteration, the values of weighted variances are updated using Equation (31). Here the objective function $f_j(j = 1, \ldots m)$ adjoined to the subspace $x_i(i = 1, \ldots n)$ is used to calculate σ_i.

7.0 NUMERICAL RESULTS

The parameters of the new optimal fuzzy two-phase CLOS guidance law, proposed in this paper, are tuned through an optimisation process. These parameters include $S_{1,\mathrm{PM}}$, $U_{1,\mathrm{PM}}$, η_1, λ_M, $S_{2,\mathrm{PM}}$, $U_{2,\mathrm{PM}}$, η_2, $K_{p,max}$, $K_{i,max}$, e_{max}, $\dot{e}_{max}$, and t_S. The performance of the new guidance law is then evaluated through different engagement scenarios. The same guidance structures, as described in Sections 3-5, are utilised for both elevation and azimuth angle control channels. Pareto CACS is utilised to optimise the parameters of the pre-constructed guidance scheme.

Ten different randomly generated engagement scenarios are used to evaluate the cost functions corresponding to each design point discovered by the ants. Two cost functions are used to optimise the parameters. The first one is the average of the total acceleration requirements over the considered engagement scenarios. The total acceleration requirement is defined as follows:

$$a_c = \int_0^{t_f} \left(a_{yc}^2 + a_{zc}^2\right)^{1/2} \mathrm{d}t \qquad \ldots (32)$$

and the average of the total acceleration requirements is defined as follows:

$$\bar{a}_c = \left(\frac{1}{10}\left(a_{c_1}^2 + a_{c_2}^2 + \ldots + a_{c_{10}}^2\right)\right)^{1/2} \qquad \ldots (33)$$

The optimisation parameters corresponding to the above cost function are categorised as follows:

$$E_1 = \{S_{1,\mathrm{PM}}, U_{1,\mathrm{PM}}, \eta_1, \lambda_M, t_S, t_{2,min}\} \qquad \ldots (34)$$

The second cost function is the average of the normalised tracking errors, evaluated over the considered engagement scenarios. The normalised tracking error is defined as follows:

$$r_n = \frac{1}{t_f - (t_{f,min} - t_{2,min})} \int_{t_{f,min} - t_{2,min}}^{t_f} r(t)\,\mathrm{d}t \qquad \ldots (35)$$

where $r(t)$ is the distance between the missile and the LOS at time t. The average of the normalised tracking errors over the scenarios, is defined as follows

$$\bar{r}_n = \left(\frac{1}{10}\left(r_{n_1}^2 + r_{n_2}^2 + \ldots + r_{n_{10}}^2\right)\right)^{1/2} \qquad \ldots (36)$$

The optimisation parameters corresponding to the second cost function are categorised as follows:

$$E_2 = \{S_{2,\mathrm{PM}}, U_{2,\mathrm{PM}}, \eta_2, K_{p,max}, K_{i,max}, e_{max}, \dot{e}_{max}\} \qquad \ldots (37)$$

The optimisation problem can be summarised as finding the optimum values of the parameter sets E_1 and E_2 such that the cost functions $\bar{a}_c$ and $\bar{r}_c$ are minimised.

Table 4
The variation of thrust and mass *versus* time

Time (sec)	Thrust (N)	Mass (kg)
0	80,000	600
4	15,000	400
20	15,000	300
23	0	300

Table 5
The variation of C_{D_0} and K *versus* Mach number

M	C_{D_0}		K
	Without based drag	With based drag	
0	0·3	0·5	0·04
0·8	0·2	0·4	0·025
1·2	0·5	0·7	0·035
2	0·35	0·55	0·04
3	0·275	0·475	0·05

7.1 Simulation model

The values of cost functions are calculated based on the missile-target engagement simulation. Under the assumption A2, the motion of the missile in the inertial frame can be represented by[7]

$$\begin{cases} \ddot{x}_m = a_{mx}\mathrm{C}\theta_m\mathrm{C}\psi_m - a_{my}(\mathrm{S}\phi_{mc}\mathrm{S}\theta_m\mathrm{C}\psi_m + \mathrm{C}\phi_{mc}\mathrm{S}\psi_m) \\ \qquad - a_{mz}(\mathrm{C}\phi_{mc}\mathrm{S}\theta_m\mathrm{C}\psi_m - \mathrm{S}\phi_{mc}\mathrm{S}\psi_m) \\ \ddot{y}_m = a_{mx}\mathrm{C}\theta_m\mathrm{S}\psi_m - a_{my}(\mathrm{S}\phi_{mc}\mathrm{S}\theta_m\mathrm{S}\psi_m - \mathrm{C}\phi_{mc}\mathrm{C}\psi_m) \\ \qquad - a_{mz}(\mathrm{C}\phi_{mc}\mathrm{S}\theta_m\mathrm{S}\psi_m + \mathrm{S}\phi_{mc}\mathrm{C}\psi_m) \\ \ddot{z}_m = a_{mx}\mathrm{S}\theta_m + a_{my}\mathrm{S}\phi_{mc}\mathrm{C}\theta_m + a_{mz}\mathrm{C}\phi_{mc}\mathrm{C}\theta_m - \mathrm{g} \\ \dot{\psi}_m = (a_{my}\mathrm{C}\phi_{mc} - a_{mz}\mathrm{S}\phi_{mc})/(v_m\mathrm{C}\theta_m) \\ \dot{\theta}_m = (a_{my}\mathrm{S}\phi_{mc} + a_{mz}\mathrm{C}\phi_{mc} - \mathrm{g}\mathrm{C}\theta_m)/v_m \end{cases} \qquad \ldots (38)$$

Where a_{mx} is the axial acceleration of missile given by $a_{mx} = (T - D)/M$. Table 4 shows the variation of thrust (T) and mass (M) *versus* time for a typical surface-to-air missile studied in this paper. The instantaneous drag force is calculated as

$$D = \frac{1}{2}\rho\, v_M^2 S C_D \qquad \ldots (39)$$

Here the standard atmosphere is used to calculate the air density (ρ) and drag coefficient (C_D) is calculated as follows

$$C_D = C_{D_0}(\mathrm{M}) + K(\mathrm{M})C_L^2 \qquad \ldots (40)$$

Where C_{D_0} and K are functions of Mach number (M). These parameters are tabulated in Table 5. The lift coefficient (C_L) is also calculated from

$$C_L = \frac{2M(a_{my}^2 + a_{mz}^2)^{0.5}}{\rho v_m^2 S} \qquad \ldots (41)$$

The same dynamic model is utilised for the target. Assuming no axial acceleration and roll motion, the simplified dynamics of target motion in the inertial frame can also be represented as follows

$$\begin{cases} \ddot{x}_t = -a_{ty}\mathrm{S}\psi_t - a_{tz}\mathrm{S}\theta_t\mathrm{C}\psi_t \\ \ddot{y}_t = a_{ty}\mathrm{C}\psi_t - a_{tz}\mathrm{S}\theta_t\mathrm{S}\psi_t \\ \ddot{z}_t = a_{tz}\mathrm{C}\theta_t - \mathrm{g} \\ \dot{\psi}_t = a_{ty}/(v_t\mathrm{C}\theta_t) \\ \dot{\theta}_t = (a_{tz} - \mathrm{g}\mathrm{C}\theta_t)/v_t \end{cases} \qquad \ldots (42)$$

https://doi.org/10.1017/S0001924000004802 Published online by Cambridge University Press

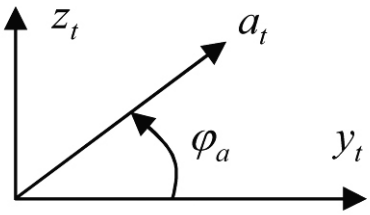

Figure 10. Definition of the target lateral manoeuver in the *y-z* plane of the body frame.

Table 6
Sample data used in simulations

Parameter	Value	Parameter	Value
f_c (Hz)	50	λ_S	5
ζ	0·6	$\boldsymbol{k}^{\mathrm{T}}$	[1 1]
ω_n (rad/s)	6π	**Q**	$\begin{bmatrix}1&0\\0&1\end{bmatrix}$
$S(m^2)$	0·1	a	0·9
ϕ_{mc}	0	d_m^u	$2a_{c,max}$
$a_{c,max}$	20g	f^u	$47\lvert\dot{e}\rvert$
δ (degree)	5	g_L	0·00003

Table 7
The initial conditions of the primary random engagement scenarios

Parameter / Scenario No.	Value 1	2	3	4	5	6	7	8	9	10
$x_t(m)$	22,501	34,929	24,614	38,013	21,066	28,967	30,825	34,905	28,670	34,192
$y_t(m)$	13,973	–11,889	–24,520	20,558	–18,017	24,550	6,962·7	–14,369	–27,061	8,302·7
$z_t(m)$	16,846	25,769	15,874	21,345	16,771	23,479	18,269	24,157	24,242	28,941
$\dot{x}_t(m/s)$	–129·34	–528·29	–438·43	–658·58	–642·99	–479·99	–573·35	–599·27	–448·55	–399·32
$\dot{y}_t(m/s)$	–398·96	7·903	360·49	–142·68	36·43	–233·51	8·4935	–120·84	24·883	–66·866
$\dot{z}_t(m/s)$	–62·956	–39·693	–65·967	25·17	57·327	–52·98	53·445	32·775	3·9051	–53·879
ψ_t (deg)	252·04	179·14	140·57	192·22	176·76	205·94	179·15	191·4	176·82	189·51
θ_t (deg)	–8·5369	–4·2963	–6·6292	2·1391	5·0867	–5·6683	5·3249	3·0688	0·49805	–7·58
$x_m(m)$	731·44	750·47	616·38	764·08	637·4	612·57	830·96	767·74	591·84	727·19
$y_m(m)$	388·62	–300·71	–635·85	437·82	–557·19	545·32	189·67	–327·07	–596·57	194·86
$z_m(m)$	560·32	588·53	464·52	473·8	532·22	572·17	523	551	542·06	658·19
$\dot{x}_m(m/s)$	219·43	225·14	184·91	229·23	191·22	183·77	249·29	230·32	177·55	218·16
$\dot{y}_m(m/s)$	116·59	–90·213	–190·75	131·35	–167·16	163·6	56·901	–98·122	–178·97	58·457
$\dot{z}_m(m/s)$	168·1	176·56	139·36	142·14	159·67	171·65	156·9	165·3	162·62	197·46
ψ_m (deg)	27·982	–21·836	–45·891	29·813	–41·159	41·676	12·858	–23·075	–45·228	15
θ_m (deg)	34·078	36·053	27·679	28·282	32·156	34·902	31·534	33·435	32·824	41·162
φ_a (deg)	129·8	4·8603	272·5	51·257	298·17	39·175	198·06	66·848	344·38	145·43
$t_{go,man}(s)$	7·6935	8·275	6·176	7·2621	6·7025	9·1912	5·5405	7·0607	5·4897	8·7568

Table 8
The initial conditions of the secondary random engagement scenarios

Parameter / Scenario No.	Value 1	2	3	4	5	6	7	8	9	10
$x_t(m)$	33,384	23,922	32,182	26,099	33,640	30,305	20,107	34,512	33,158	31,639
$y_t(m)$	96,48·8	12,342	14,612	–13,792	–24,885	–19,875	–19,538	–22,494	–15,971	–9,970·1
$z_t(m)$	14,145	19,842	14,062	17,398	16,712	28,398	13,009	17,883	20,275	18,616
$\dot{x}_t(m/s)$	–528·25	–477·04	–394·14	–576·09	–270·13	–405·44	–119·15	–567·11	–546·57	–339·13
$\dot{y}_t(m/s)$	24·191	143·95	–214·99	87·844	414·98	281·12	608·77	–30·715	–10·656	547·34
$\dot{z}_t(m/s)$	23·528	–54·737	38·761	34·139	58·223	–55·042	–12·826	–62·494	–89·821	34·492
ψ_t (deg)	177·38	163·21	208·61	171·33	123·06	145·26	101·07	183·1	181·12	121·78
θ_t (deg)	2·5475	–6·2689	4·9343	3·3527	6·7062	–6·3659	–1·1845	–6·2794	–9·3306	3·0663
$x_m(m)$	874	667·81	846·56	744·81	750·43	646·12	645·51	752·53	771·58	814·29
$y_m(m)$	277·85	398·1	377·95	–429·17	–504·67	–368·43	–595·52	–492·34	–393·03	–251·11
$z_m(m)$	398·65	628·92	374·83	510·96	426·8	668·42	478·2	437·38	500·19	523·33
$\dot{x}_m(m/s)$	262·2	200·34	253·97	223·44	225·13	193·84	193·65	225·76	231·47	244·29
$\dot{y}_m(m/s)$	83·356	119·43	113·38	–128·75	–151·4	–110·53	–178·65	–147·7	–117·91	–75·332
$\dot{z}_m(m/s)$	119·59	188·68	112·45	153·29	128·04	200·53	143·46	131·21	150·06	157
ψ_m (deg)	17·636	30·8	24·059	–29·951	–33·921	–29·693	–42·693	–33·195	–26·994	–17·138
θ_m (deg)	23·494	38·971	22·014	30·728	25·265	41·946	28·568	25·937	30·013	31·556
φ_a (deg)	127·2	283·2	183·81	136·16	28·469	160·8	83·297	153·21	107·71	26·922
$t_{go,man}(s)$	6·7996	5·7585	9·5913	8·4281	6·3441	9·5381	6·8227	8·8922	5·8699	7·4291

A step target manouever[3] in the form of a lateral acceleration command with constant magnitude, random direction and random initiation time is utilised in the simulations. The positive direction of the target lateral acceleration is shown in Fig. 10. The pitch and yaw autopilot dynamics are chosen as the second-order time invariant. The detailed data, used in simulations, are listed in Table 6.

7.2 Generation of the random engagement scenarios

The cost functions, corresponding to each design point, are evaluated based on the average performance obtained over ten randomly generated engagement scenarios. These scenarios are pre-generated because the same situations are needed to evaluate different design

https://doi.org/10.1017/S0001924000004802 Published online by Cambridge University Press

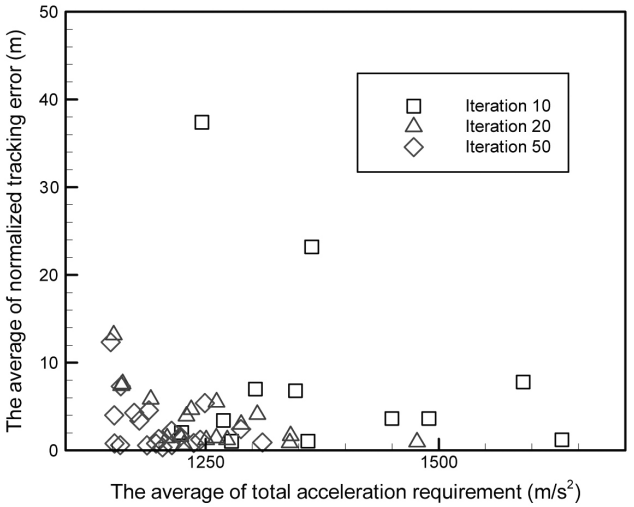

Figure 11. The history of the Pareto-optimal set.

points. In the generation of these primary scenarios, the following constraints are assumed

$$\begin{cases} 30{,}000 \le R_{0t} \le 50{,}0 \\ -45^\circ \le \sigma_{0t} \le 45^\circ \\ 20^\circ \le \gamma_{0t} \le 40^\circ \end{cases}, \begin{cases} 400 \le v_{0t} \le 700 \\ -45^\circ \le \psi_{0t} \le 45^\circ \\ -10^\circ \le \theta_{0t} \le 10^\circ \end{cases}, \begin{cases} R_{0m} = 1000\ m \\ -5^\circ \le \sigma_{0m} - \sigma_{0t} \le 5^\circ, \\ -5^\circ \le \gamma_{0m} - \gamma_{0t} \le 5^\circ \end{cases}$$

$$\begin{cases} v_{0m} = 300\ ms^{-1} \\ \psi_{0m} = \sigma_{0m} \\ \theta_{0m} = \gamma_{0m} \end{cases}, \begin{cases} 0 \le \varphi_a \le 360^\circ \\ 5 \le t_{go,man} \le 10 \end{cases}$$

Here $t_{go,man}$ is the estimated time-to-go when the random step manoeuvre is applied. Two different sets of random engagement scenarios are provided, a primary set to be used in the optimisation process, and a secondary set to evaluate the performance of the optimised guidance law. The parameters of these two sets are listed in Tables 7 and 8.

7.3 Optimisation results

The optimisation algorithm searches among different points of the solution space in an intelligent stochastic manner. The evaluation is done through the simulation of the missile-target engagement for the given primary scenarios. The boundaries of the search space are chosen as follows

$$0 < S_{1,PM} < 1,\ 0 < U_{1,PM} < 1,\ 0 < \eta_1 < 10,\ 0 < \lambda_M < 10,$$

$$2 < \xi < 10,\ 2 < t_{2min} < 10$$

$$0 < S_{2,PM} < 1,\ 0 < U_{2,PM} < 1,\ 0 < \eta_2 < 0.1,$$

$$0 < K_{p,max} < 10,\ 0 < K_{i,max} < 10,\ 0 < e_{max} < 1,\ 0 < \dot{e}_{max} < 1$$

An important aspect of CACS with respect to the other meta-heuristic optimisation methods is its fewer number of control parameters[32,33]. CACS has only one parameter to set, which is the number of ants (k). According to the previous experiences[16,32,33], the value of $k = 10$ has been found as the best solution that works well over a wide range of analytical and engineering problems. The same setting is adopted in this paper.

Table 9
A statistical study over the history of the Pareto-optimal set

Iteration number	Percentage of the solutions within the range		
	$c_1 < 1{,}500$, $c_2 < 50$	$c_1 < 1{,}300$, $c_2 < 20$	$c_1 < 1{,}200$, $c_2 < 10$
10	50%	15%	0%
20	90%	70%	15%
50	100%	95%	50%

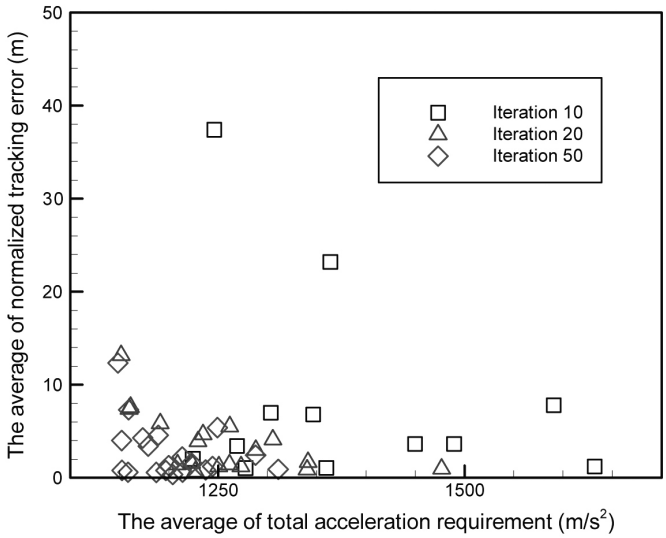

Figure 12. The selection of the final design point within the best solutions.

With the design problem and parameters completely defined, PCACS was executed several times. The solution of each run is a Pareto-optimal solution. Thus the solutions obtained from different runs provide a Pareto-optimal set. Figure 11 shows the history of the Pareto-optimal set, obtained from 20 different runs. The maximum number of evaluations is limited to 500 per run. The history of the Pareto-optimal set is shown in three different snapshots corresponding to the iterations 10, 20 and 50.

A statistical study over the history of the Pareto-optimal set is made. Table 9 shows the percentage of the solutions, found within the specified ranges of the cost functions. The represented data can also be used to choose an efficient value for the maximum number of iterations. It can easily be found that if designer is interested in the solutions where $c_1 < 1{,}500$ and $c_2 < 50$, its better to stop after ten iterations and use 100 runs as apposed to stop after 20 iterations and using 50 runs. Both cases include 1,000 evaluations, but in the first case 50 solutions (out of 100 solutions) will be obtained within the range, while in the second case only 45 solutions (out of the total 50 solutions) will be obtained within the range. The same analysis shows that to investigate the solutions where $c_1 < 1{,}300$ and $c_2 < 20$, it's better to stop after 20 iterations instead of ten or 50.

The final solutions are zoomed in Fig. 12. Each point corresponds to a design point. Considering the fact that it is more important to reduce tracking error than the acceleration command, a final design point is chosen, as shown in Fig. 12. The history of the cost functions, corresponding to the final design point, is shown in Fig. 13. The optimum values of the parameters, obtained after 500 evaluations (50 iterations), are $S_{1,PM} = 0{\cdot}28$, $U_{1,PM} = 0{\cdot}01$, $\eta_1 = 1{\cdot}96$, $\lambda_M = 9{\cdot}78$, $t_S = 9{\cdot}69$, $t_{2,min} = 7{\cdot}82$, $S_{2,PM} = 0{\cdot}10$, $U_{2,PM} = 0{\cdot}72$, $\eta_2 = 0{\cdot}20$, $K_{p,max} = 1{\cdot}2$, $K_{i,max} = 6{\cdot}10$, $e_{max} = 0{\cdot}04$, $\dot{e}_{max} = 0{\cdot}14$.

https://doi.org/10.1017/S0001924000004802 Published online by Cambridge University Press

Table 10
evaluation of the optimal design against the secondary scenarios

Scenario	Current study		Feedback linearisation	
	Acceleration requirement	Miss distance (m)	Acceleration requirement	Miss distance (m)
1	1,089	0·514	1,290	1·161
2	817	2·466	1,084	1·92
3	965	1·898	1,067	0·516
4	1,227	0·840	1,378	1·714
5	1,134	0·855	1,502	0·320
6	1,332	0·889	1,487	0·649
7	1,259	0·320	1,544	1·609
8	1,227	0·536	1,402	2·006
9	1,130	0·458	1,295	0·910
10	1,470	0·516	1,638	0·477
average	1,178	1·142	1,380	1·282

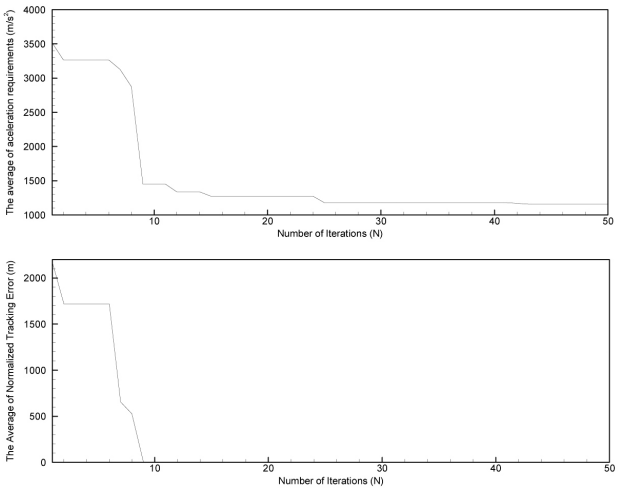

Figure 13. The history of the cost functions corresponding to the final design point.

7.4 Evaluation of the optimal design

In this section the optimal set of parameters, determined based on the primary engagement scenarios (learning scenarios), are evaluated against the secondary scenarios (test scenarios). The simulation results are represented in Table 10 and compared with those of a model-based feedback linearisation (FBL) method[7]. FBL is chosen for evaluation of the results, since it is known as a high performance CLOS guidance for medium range missile compatible with our current case. It should be noted that the other state-of-the-art CLOS guidance laws proposed in Refs 12-16 show good performances in the cases of short range missiles. However, the performance of these approaches degrades for medium range interceptions, partly because they have been designed for small miss distances not small control efforts.

The performance evaluation scheme consists of the total acceleration requirement and the final miss distance. Table 10 shows that the performance of the optimal fuzzy two-phase (OFTP) CLOS guidance scheme is relatively better than those of FBL.

One important aspect of OFTP is the fewer information and consequently hardware requirements needed to calculate the acceleration commands. Table 11 compares the information requirements between OFTP and FBL. Both methods need a continuous measurement of $\Delta\sigma$ and $\Delta\gamma$. This information can be obtained from a differential tracking system. It is also required to have approximate values for the initial range and velocity of target. The operator uses this information to decide whether to fire against a given target or not. Moreover, OFTP uses this information to estimate $t_{f,min}$. That is all for OFTP. However, FBL needs additional measurements of σ_t, γ_t, $\dot{\sigma}_t$, $\dot{\gamma}_t$, R_m, ψ_m and θ_m. The first four parameters can be measured by the tracking system, while an inertial navigation system (INS) is required to measure the later three parameters.

Table 11
A comparison between the information requirements of OFTP and FBL

Information parameter	Measurement/ Estimation source	Requirements	
		OFTP	FBL
$\Delta\sigma$, $\Delta\gamma$	Tracker	√	√
$x_t(0)$, $y_t(0)$, $z_t(0)$ $\dot{x}_t(0)$, $\dot{y}_t(0)$, $\dot{z}_t(0)$	Search radar/ radar network	√	√
σ_t, γ_t, $\dot{\sigma}_t$, $\dot{\gamma}_t$	Tracker	×	√
R_m, ψ_m, θ_m	Inertial navigation system	×	√
$\Delta\dot{\sigma}$, $\Delta\dot{\gamma}$	Band limited differentiators	√	×
$\ddot{\sigma}_t$, $\ddot{\gamma}_t$, $\dot{R}_{LOS}$, $\dot{R}_y$, $\dot{R}_z$	Band limited differentiators	×	√
a_{xm}	Experimental aero-data	×	√

Table 11 also shows that OFTP needs fewer band limited differentiators than FBL. Another requirement of FBL is the time profile of the missile axial acceleration, estimated from the experimental aero-data. It is not the case for OFTP.

The simulation results for a sample scenario (the first scenario of Table 8) are plotted in Figs 14 and 15 corresponding to OFTP and FBL, respectively. These include missile and target trajectories, tracking behaviour in elevation and azimuth channels, acceleration commands and target acceleration.

Although OFTP uses the least information, Fig. 14 shows that this new guidance law, designed using PCACS, can successfully guide the missile toward the target with a good performance. The way the missile is being guided with a lead angle with respect to the LOS and the way this lead angle vanishes, are shown in Fig. 14(c,d). Contrary to OFTP, FBL immediately drives the missile toward the LOS (Fig. 15(c,d)). The time histories of the missile and target accelerations in pitch and yaw channels are shown in Figs 14 and 15(e,f). It can be observed that FBL demands more control effort during the initial times as compared with OFTP. In turn, OFTP shows a similar behaviour during the shaping phase. The acceleration demands are similar for both strategies during the target manoeuvre. It can also be observed that OFTP has a relatively smoother control effort as compared with FBL.

The performance of the new guidance law is also evaluated in the presence of measurement noise. Here the proposed model of Table 8 is used to simulate measurement noise of missile and target lines-of-sight. This model is shown in Fig. 16. Table 12 compares the performance of OFTP and FBL in the presence of LOS noise. Although the performance is slightly degraded, they indicate that both OFTP and FBL can successfully deal with measurement noise. However,

https://doi.org/10.1017/S0001924000004802 Published online by Cambridge University Press

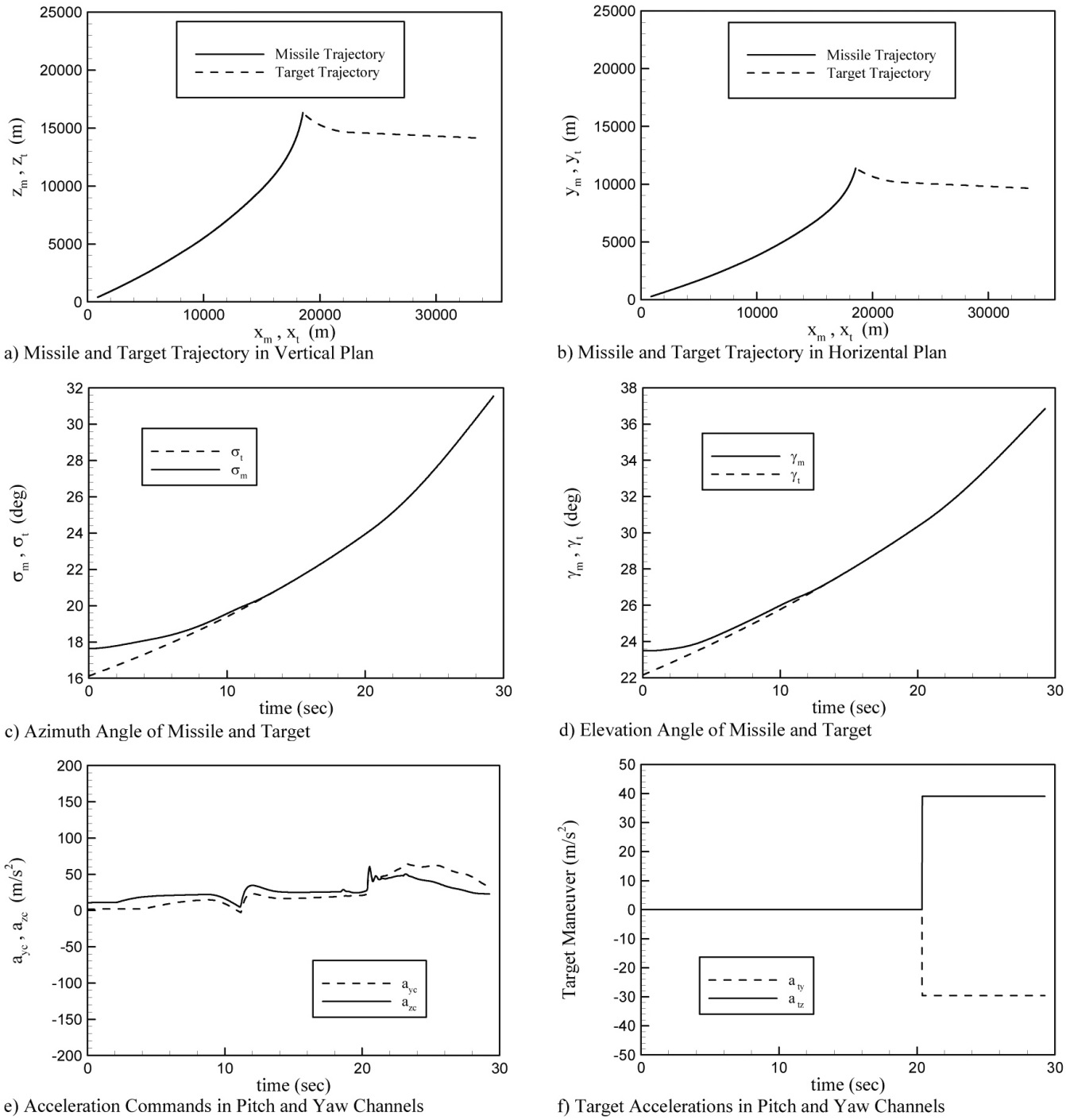

Figure 14. Engagement simulation of OFTP for the first scenario of Table 8.

OFTP shows to be less influenced by noise as compared with FBL. In fact since the control effort is one of the cost functions considered, it causes the optimisation algorithm to search for the solutions with minimum control effort. This is the main reason for which OFTP shows lower sensitivity to measurement noise.

For the first scenario of Table 8, the acceleration commands of OFTP and FBL in the presence of noise are shown in Fig. 17 and Fig. 18, respectively. The comparison of these two figures shows the better performance of OFTP. It should be noted that OFTP is not sensitive to noise in the first guidance phase, while FBL is showing sensitivity to noise during the total flight time.

8.0 CONCLUSION

A new optimal fuzzy two-phase (OFTP) CLOS guidance law was designed using ant colony optimisation (ACO). The new guidance scheme utilises a lead angle strategy in a portion of flight and does not require a continuous estimation of time-to-go. The guidance problem is divided into two phases, a midcourse and a terminal phase. In the first phase, the missile is guided with a lead angle with respect to LOS, using approximate information on time-to-go. In this phase, a PD fuzzy sliding mode controller is used as the main tracking controller. Moreover, a supervisory controller is coupled

https://doi.org/10.1017/S0001924000004802 Published online by Cambridge University Press

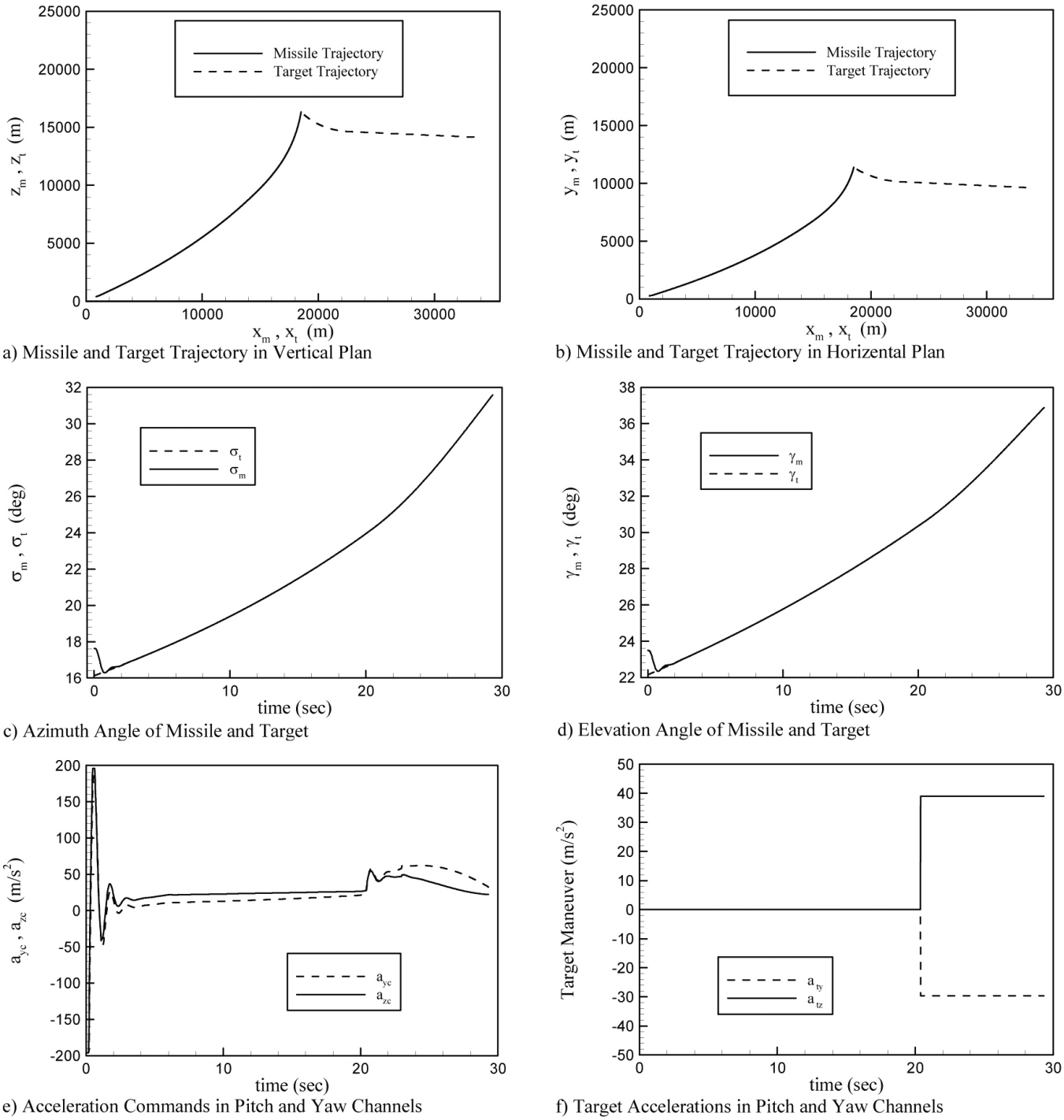

Figure 15. Engagement simulation of FBL for the first scenario of Table 8.

with the main tracking controller to guarantee the missile flight within the beam. In the terminal phase, a pure CLOS guidance law without lead angle is utilised. For this phase, a new hybrid fuzzy PID fuzzy sliding mode controller was proposed as a high precision tracking controller. The recently developed continuous ant colony system (CACS) algorithm, which is based on ACO, was extended to multi-objective optimisation problems. The new optimisation algorithm, called PCACS, was applied to optimise the parameters of the pre-constructed fuzzy controllers. A statistical study was also made to choose the final design point.

The performance of the designed guidance law was evaluated at different engagement scenarios and compared with a model-based feedback linearisation (FBL) CLOS guidance law. The effect of LOS measurement noise was also studied in simulations. The obtained results show that OFTP can successfully guide the missile toward the target with an acceptable performance. The results of OFTP are relatively better than those of FBL, especially in the presence of measurement noise. An important aspect of OFTP is its least information requirement. The proposed methodology does not require any information obtained from the inertial navigation system,

https://doi.org/10.1017/S0001924000004802 Published online by Cambridge University Press

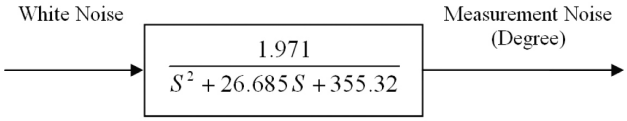

Figure 16. Model used to produce missile and target LOS noise.

Table 12
Evaluation of the secondary scenarios in the presence of LOS noise

Scenario	Current study		Feedback linearisation	
	Acceleration requirement $(m/s)^2$	Miss distance (m) (m)	Acceleration requirement $(m/s)^2$	Miss distance (m) (m)
1	1,091·6	0·76083	1,309·9	1·5121
2	820·92	2·0687	1,108·5	2·1866
3	968·83	1·9611	1,093·4	1·0204
4	1,228·6	1·121	1,387·4	1·6829
5	1,141·5	1·1602	1,538·4	0·42794
6	1,356·5	1·3692	1,525·7	1·3419
7	1263·0	0·56344	1,552·9	1·6474
8	1,228·3	0·90707	1,433·1	2·0272
9	1,136·9	0·56396	1,316.0	2·0034
10	1,472·1	0·5963	1,652·9	0·34023
average	1,184·1	1·2246	1,403·2	1·5452

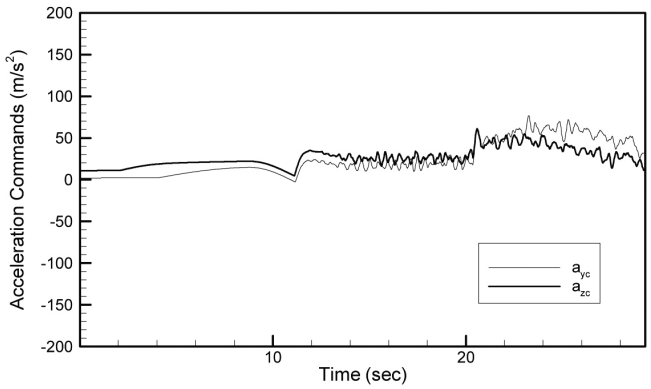

Figure 17. Acceleration commands of OFTP in the presence of measurement noise.

while FBL does. Moreover OFTP contains less differentiation operations compared with FBL.

The results also verify the potential of PCACS to solve practical design optimisation problems such as guidance and control systems design.

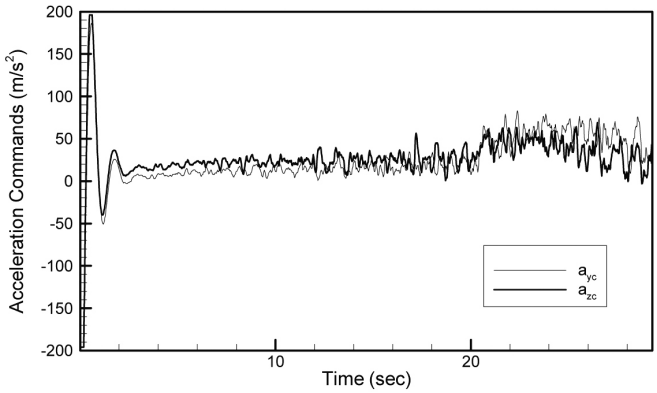

Figure 18. Acceleration commands of FBL in the presence of measurement noise.

REFERENCES

1. LOCKE, A.S. *Guidance*, 1955, D. Van Nostrand Company, Princeton.
2. GARNELL, P., *Guided Weapon Control Systems*, 1980, Second edition, Pergamon Press, Oxford, UK.
3. ZARCHAN, P. *Tactical and Strategic Missile Guidance*, 1997, Third edition, AIAA Education Series, Vol 176, AIAA.
4. BLACKELOCK, J.H. *Automatic Control of Aircraft and Missiles*, 1991, Second edition, New York, Wiley.
5. SHNEYDOR, N.A. *Missile Guidance and Pursuit: Kinematics, Dynamics and Control*, Horwood Publishing, Chichester, England, UK, 1998.
6. KAIN, J.E. and YOST, D.J. Command to line-of-sight guidance: a stochastic optimal control problem, AIAA Guidance and Control conference proceedings, 1976, pp 356-364.
7. HA, I.J. and CHONG, S. Design of a CLOS Guidance law via feedback linearization, 1992, IEEE Transactions on Aerospace and Electronic Systems, **28**, (1), pp 51-62.
8. PARKES, N.E. and ROBERTS, A.P. Application of polynomial methods to design of controllers for CLOS guidance, 1994, IEEE Conference on Control Applications, **2**, pp 1453-1458.
9. BENSHABAT, D.G. and BAR-GILL, A. Robust command-to-line-of-sight guidance via variable-structure control, 1995, IEEE Transactions on Control Systems Technology, **3**, (3), 1995, pp 356-361.
10. POURTAKDOUST, S.H. and NOBAHARI, H. Optimization of LOS guidance for surface-to-air missiles, September 2000, Proceedings of Iranian Aerospace Organization Conference, Tehran, pp 245-257.
11. NOBAHARI, H., ALASTY, A. and POURTAKDOUST, S.H. Design of a supervisory controller for CLOS guidance with lead angle, AIAA Guidance, Navigation and Control Conference and Exhibition, AIAA 2005-6156, pp 1-13.
12. ARVAN, M.R. and MOSHIRI, B. Optimal fuzzy controller design for an anti-tank missile, September 1996, Proceedings of International Conference on Intelligent and Cognitive Systems, Tehran, pp 123-128.
13. LIN, C.M. and MON, Y.J. Fuzzy-logic-based CLOS guidance law design, 2001, IEEE Transactions on Aerospace and Electronic Systems, **37**, (2), pp 719-727.
14. LIN, C.M. and HSU, C.F. Guidance law design by adaptive fuzzy sliding mode control, *J Guidance, Control and Dynamics*, 2002, **25**, (2), pp 248-256.
15. LIN, C.M., HSU, C.F. and MON, Y.J. Self-organizing fuzzy learning CLOS guidance law design, 2003, IEEE Transactions on Aerospace and Electronic Systems, **39**, (4), pp 1144-1151.
16. NOBAHARI, H. and POURTAKDOUST, S.H. Optimal fuzzy CLOS guidance law design using ant colony optimization, 2005, Lecture Notes in Computer Science, 3777, pp 95-106.
17. LEE, G.T. and LEE, J.G. Improved command-to-line-of-sight for homing guidance, IEEE Transactions on Aerospace and Electronic Systems, 1995, **31**, (1), pp 506-510.
18. JALALI-NAINI, S.H. and ESFAHANIAN, V. Closed-form solution of line-of-sight trajectory for non-maneuvering targets, *J Guidance, Control and Dynamics*, 2000, **23**, (2), pp 365-366.
19. JALALI-NAINI, S.H. Analytical study of a modified LOS guidance, AIAA Guidance, Navigation and Control Conference, AIAA 2001-4045, pp 1-8.
20. JALALI-NAINI, S.H. Generalized line-of-sight guidance with lead angle, *Iranian Journal of Science and Technology*, Transaction B, 2004, **28**, (B4), pp 489-493.
21. BELKHOUCHE, F., BELKHOUCHE, B. and RASTGOUFARD, P. A Linearized model for the line-of-sight guidance law, 2004, Proceedings of IEEE Position Location and Navigation Symposium, pp 201-207.
22. WANG, L.X., A supervisory controller for fuzzy control systems that guarantees stability, 1994, IEEE Transaction on Automatic Control, **40**, (1), pp 1845-1848.
23. PALM, R. Robust control by fuzzy sliding mode, *Automatica*, 1994, **30**, (9), pp 1429-1437.

https://doi.org/10.1017/S0001924000004802 Published online by Cambridge University Press

24. CHEN, C.L. and CHANG M.H. Optimal design of fuzzy sliding-mode control: a comparative study, *Fuzzy Sets and Systems*, 1998, **93**, pp 37-48.
25. CHOI, B.J., KWAK, S.W. and KIM, B.K. Design of a single-input fuzzy logic controller and its properties, *Fuzzy Sets and Systems*, 1999, **106**, (3), pp 299-308.
26. BREHM, T. and RATTAN, K.S. Hybrid fuzzy logic PID controller, Proceedings of the IEEE National Aerospace and Electronics Conference, 1993, **2**, pp 807-813.
27. ZHAO, Z.Y., TOMIZUKA, M. and ISAKA, S. Fuzzy gain scheduling of PID controllers, 1993, IEEE Trans. Systems, *Man and Cybernetics*, **23**, pp 1392-1398.
28. PROCYK, T.J. and MAMDANI, E.H. A linguistic self-organizing process controller, *Automatica*, IFAC, 1979, **15**, pp 15-30.
29. TAKAGI, T. and SUGENO, M. Fuzzy identification of systems and its application to modeling and control, 1985, IEEE Trans. Systems, *Man and Cybernetics*, **15**, pp 116-132.
30. NOMURA, H., HAYASHI, I. and WAKAMI, N. A Self tuning method of fuzzy control by descent method, *Engineering*, 1991, Bruxelles, Proceedings of the International Fuzzy Systems Association, IFSA91, pp 155-158.
31. SIARRY, P. and GUELY, F. A genetic algorithm for optimizing Takagi-Sugeno fuzzy rule bases, *Fuzzy Sets and Systems*, 1998, **99**, pp 37-47.
32. NOBAHARI, H. and POURTAKDOUST, S.H. Optimization of fuzzy rule bases using continuous ant colony system, 2005, Proceeding of the First International Conference on Modeling, Simulation and Applied Optimization, Sharjah, UAE, **243**, pp 1-6.
33. POURTAKDOUST, S.H. and NOBAHARI, H. An extension of ant colony system to continuous optimization problems, *Lecture Notes in Computer Science*, 2004, **3172**, pp 294-301.
34. COLORNI, A., DORIGO, M. and MANIEZZO, V. Distributed optimization by ant colonies, 1992, Proceedings of the First European Conference on Artificial Life, pp 134-142.
35. DORIGO M. and GAMBARDELLA, L.M. Ant colony system: a cooperative learning approach to the traveling salesman problem, *IEEE Transactions on Evolutionary Computation*, 1997, **1**, (1), pp 53-66.
36. SLOTINE, J.J.E. and LI, W. *Applied Nonlinear Control*, 1991, Prentice-Hall, Upper Saddle River, NJ.
37. RAO, S.S. *Engineering Optimization*, 1996, John Wiley & Sons and New Age International (P).